Spatial distribution of Pleistocene/Holocene warming amplitudes in Northern Eurasia inferred from geothermal data

D. Yu. Demezhko, D. G. Ryvkin, V. I. Outkin, A. D. Duchkov, V. T. Balobaev

Clim. Past Discuss., 3, 607–630, 2007
www.clim-past-discuss.net/3/607/2007/

Climate of the Past Discussions is the access reviewed discussion forum of *Climate of the Past*

Spatial distribution of Pleistocene/Holocene warming amplitudes in Northern Eurasia inferred from geothermal data

D. Yu. Demezhko[1], D. G. Ryvkin[1], V. I. Outkin[1], A. D. Duchkov[2], and V. T. Balobaev[3]

[1]Institute of Geophysics, UB RAS, Ekaterinburg, Russia
[2]Institute of Geophysics, SB RAS, Novosibirsk, Russia
[3]Institute of Permafrost Studies, SB RAS, Yakutsk, Russia

Received: 28 February 2007 – Accepted: 1 March 2007 – Published: 15 March 2007

Correspondence to: D. Yu. Demezhko (ddem54@inbox.ru)

Abstract

We analyze 48 geothermal estimates of Pleistocene/Holocene warming amplitude from various locations in Greenland, Europe, Arctic regions of Western Siberia, and Yakutia. The spatial distribution of these estimates exhibits two remarkable features. (i) In Europe and part of Asia the amplitude of warming increases towards northwest and displays clear asymmetry with respect to the North Pole. The region of maximal warming is close to the North Atlantic. A simple parametric dependence of the amplitude on the distance to the warming center explains 91% of the amplitude variation. The Pleistocene/Holocene warming center is located northeast of Iceland. We claim that the Holocene warming is primarily related to the formation (or resumption) of the modern system of currents in the North Atlantic. (ii) In Arctic Asia, north of the 68-th parallel, the amplitude sharply decreases from South to North, reaching zero and even negative values. Too small amplitudes could be attributed to a joint warming influence of Late Pleistocene ice sheets and warm-water lakes formed in Late Pleistocene by the damming of the Ob, Yenisei and Lena Rivers. Using a simple model of the temperature regime underneath the ice sheet we show that, depending on the relationship between the heat flow and the vertical ice advection velocity, the base of the glacier can either warm up or cool down.

1 Introduction

Reconstruction of past climate changes is instrumental in understanding and forecasting contemporary climate. The last most significant natural climate change happened on the edge of Pleistocene and Holocene (13-8 thousand years back). At that time the climate system was undergoing a transition from one quasi-stable state (glaciation) to another (interglacial). Reconstruction of the spatial structure of Pleistocene/Holocene warming (PHW) can geographically locate the initialization centers of the positive feedback mechanism eventually leading to the global climate change.

In the present study we estimate the spatial distribution of PHW amplitudes in Northern Eurasia using geothermal data. In prior work, Huang et al. (1997) and Kukkonen and Joeleht (2003) obtained long averaged temperature histories for the whole world and East-European Platform (including Fennoscandia), respectively. Both studies used the Global Heat Flow Data Base of the International Heat Flow Commission of IASPEI (Pollack et al., 1993). The estimated Pleistocene/Holocene global warming was less than 1.5 K (Huang et al., 1997) and 8±4.5 K (Kukkonen and Joeleht, 2003). Our claim is that both studies significantly underestimated the warming. In particular, Demezhko et al. (2005) have shown that the omitted variation in thermal conductivity of bedrock (this information is absent in the database mentioned above) leads to a disagreement in the dates of the extrema of the reconstructed climate histories. Averaging of histories and/or joint inversion may lead to lower estimates of the average amplitude of temperature variations. Individual estimation of PHW amplitudes using separate qualitative temperature-depth profiles is more reliable. Generally, a complete spatial distribution has to contain more paleoclimatic information than any average estimates.

2 Geothermal estimates of PHW amplitudes

For our analysis we use two groups of geothermal estimates for Northern Eurasia obtained by different authors (Fig. 1). The first group contains the estimates of PHW amplitudes in Europe and in the Urals and also the estimate of warming amplitude on the surface of the Greenland Ice Sheet. For those datasets which include a detailed ground surface temperature history, we estimated the PHW amplitude as the difference in average temperatures over the periods of 30-15 thousand years back (Late Pleistocene) and 8-0 thousand years back (Holocene).

The second group of geothermal estimates (Table 2) characterizes the changes in surface temperature in the northern part of Western Siberia, and in Yakutia. In these regions, non-stationary melting of Pleistocene permafrost has a significant impact on heat transfer. We estimated the paleotemperatures by solving the non-stationary heat

equation with Stefan condition at the phase boundary with an approximate numerical/graphical algorithm (Balobaev, 1991).

3 Spatial distribution of PHW amplitude

The range of estimates – from −2 K in the lower Lena River to +23 K on the Greenland Ice Sheet – points at significant and controversial changes in the surface temperature on the edge of Pleistocene and Holocene.

The spatial distribution of PHW amplitudes (Fig. 2) has the following features. (1) In the Urals and west of them the amplitude increases in the northwest direction. Isoanomaly ΔT_s=+10 K is descending from 65° N at the 80° E meridian to 57° N at 60° E and to 47° N at the 20° E meridian. East of the 80° meridian the ΔT_s=+10 K isoanomaly stays practically flat. Isoanomaly ΔT_s=+20 K embraces Fennoscandia in the Southeast and tends northwest towards Greenland. (2) The regular pattern is violated by some of Western Siberia and Yakutia estimates, for which the amplitude decreases northward of 68° N. The amplitude falls to 3-0 K at the Yamal peninsula and becomes negative, −2 K, in the lower Lena River (i.e. here the surface temperature dropped and the permafrost thickness increased by 40 m since the glaciation period, see Table 2). We believe that the origin of this deviation is unrelated to climate; there had to be another warming factor at work for a long time.

The isoanomalies in Fig. 2 are very imprecise: for the small sample of data used, their shape depends considerably on the interpolation method. Clearly, however, the isoanomalies have a saturation point – a center of warming located in the North Atlantic. The coordinates of this hypothetical center can be estimated with a higher precision if one adopts a parametric mathematical model for the distribution of warming. In the present paper we do not discuss any specific mechanisms of heat transfer; instead, we test several very simple (but still, physically somewhat meaningful) models.

Consider functions of the form

$$\Delta T_i(r_i) = k_1 + k_2 r_i^m, \quad r_i = r(\varphi_0, \lambda_0, \varphi_i, \lambda_i), \tag{1}$$

where r_i is the distance from the center of warming with coordinates φ_0 (latitude) and λ_0 (longitude) to a data point i with coordinates φ_i, λ_i, (i=1,2...n). at which the warming amplitude ΔT_i is reconstructed; k_1 and k_2 are constants; exponent m=1, −1, −2 determines the functional form. Exponent m=−1 is physically reasonable: it describes the heat flow from a point source in a thin flat layer with the temperature anomaly ΔT linear in the flux. A similar linear relationship between the outgoing heat flux and the surface temperature was proposed by Budyko (1980).

The optimal model parameters (φ_0, λ_0, k_1, k_2) are found by minimizing the functional

$$M = 1 - R^2 \rightarrow \min \quad (2)$$

where R^2 is the square of the linear correlation coefficient between ΔT and r^m for the chosen model. Functional M=1−R^2 characterizes the unexplained share of the total dispersion D, while $(DM)^{1/2}$ describes the mean square deviation of the model residuals.

For estimation of the position of the center of warming, the following adjustments have been made in the initial sample: closely located estimates have been merged, and the data north of 68° N removed from the sample. The adjusted sample is shown in Table 3. The estimation results for the three models are shown in Table 4.

The non-linear models S2 and S3 yield the minimal values of the functional M. The mean square deviation $(DM)^{1/2}$ can be regarded as an accuracy measure for geothermal reconstruction of the Pleistocene/Holocene warming amplitude. It is below 1.5 K for the non-linear models, which compares well with Dahl-Jensen et al. (1998) who estimate the accuracy to be 2 K in their GRIP reconstruction. The differences among the nearest boreholes are also of the order of 2 K: De-1 (11 K) and KTB (9 K); Il-1 (8 K) and Le-1 (10 K), see Table 1.

Along with the optimal position of the center of warming and the value of functional M at its minimum, it is of interest to explore the shape of the minimal functional $M(\varphi_0, \lambda_0)$ as a function of the position. Figure 3 shows the isolevel lines of $M(\varphi_0, \lambda_0)$ for M<0.5. Their elongated shape indicates that the real source of warming was signifi-

cantly different from a point source and looked more as a line source. The shape of this line approximately follows the pattern of warm currents in the North Atlantic.

Thus, the results suggest that warm currents in the North Atlantic could be a source of the PHW. Sufficiently far from the source, e.g., in Yakutia, the warming amplitude drops to 7–9 K. Here, most likely, it is not directly related to the Atlantic but determined by the reaction of the planetary climate system to the initial regional warming.

The results of our modeling can also be useful for traditional geothermal problems, in particular, for finding paleoclimatic corrections to the measured heat flow density. The PHW distorts the heat flow for depths up to ~2.5 km. For depths up to ~500 m this distortion is complemented by the Holocene climate changes. Therefore, the distribution of PHW amplitudes shown in Fig. 4 can be used to calculate the paleoclimatic corrections in the interval 500–2500 m.

4 Derivation from the regular pattern

A number of geothermal PHW estimates for Western Siberia and Yakutia north of the 68th parallel deviate significantly from the regular pattern identified (Fig. 2). Northward, the warming amplitudes quickly decrease to 3-0 K at the Yamal Peninsula and to −2 K in the lower Lena River. Thus, the Late Pleistocene surface temperature in these regions was only slightly below and, in some case, even above the temperature today. This observation points at the existence of a warming source that was affecting the surface for a long time.

4.1 The influence of ice sheets on the ground surface temperature

One possible source of the warming effect is the influence of Late Pleistocene ice sheets. According to the Panarctic Ice Sheet hypothesis (Hughes et al., 1977; Grosswald, 1996), during Late Pleistocene, Arctic Eurasia was covered by a continuous chain of glaciers. The Kara's and East-Siberian Ice Sheets were part of this region. However,

the following question may arise: if the influence of Siberian glaciers can be so easily traced in today's temperature field, why is there no similar trace of the Scandinavian Ice Sheet?

The unexpectedly high geothermal estimates of PHW amplitudes for holes on Kola peninsula (Kol, $\Delta T = 20$ K, Glaznev et al., 2004), in Karelia (Krl, $\Delta T = 18$ K, Kukkonen et al., 1998), and in Poland (Udryn, $\Delta T = 17$ K, Safanda et al., 2004) contain no indication of glacier-related warming.

In fact, a glacier's influence on the ground surface temperature is more complex. Several factors contribute to changes in the temperature under a glacier: geothermal heat flow and friction lead to the temperature increase, while vertical ice flow leads to its decrease. Surface temperature changes, in turn, affect mechanical properties of the ice. Model numerical simulations (Payne et al., 2000) show that an interplay of all these factors may lead to a thermomechanical instability, which makes it impossible to predict the basal temperature distribution.

We estimated the influence of the glacier on the surface temperature using a simple one-dimensional stationary model, which, however, takes into account the role of snow cover, an additional factor that we believe to be significant. Without a glacier, the mean annual surface temperature is determined by the air temperature and the warming influence of snow cover. This warming influence increases with the snow cover height and the amplitude of annual air temperature fluctuations, and decreases with the mean annual air temperature (Demezhko, 2001). The glacier eliminates this effect and somewhat cools the ground surface.

Consider heat transfer in an instantly emerged glacier of a finite height h, which covers a semi-infinite massif of bedrock. Let the thermal properties of the ice and the rock be constant but different. Further, let the velocity of the vertical ice flow at the glacier surface be equal to the accumulation rate, and hence the height h be constant. With the vertical axis z directed downwards, and the origin at the flat impenetrable ice/rock contact surface, the system of one-dimensional heat equations can be written

in the form

$$\begin{aligned} &\frac{\partial^2 T_i}{\partial z^2} - \frac{V_{iz}(z)}{a_i}\frac{\partial T_i}{\partial z} = \frac{1}{a_i}\frac{\partial T_i}{\partial t}, \ -h \le z \le 0 \\ &\frac{\partial^2 T_0}{\partial z^2} = \frac{1}{a_0}\frac{\partial T_0}{\partial t}, \ z > 0 \\ &V_{iz}(z) = -V_s z/h. \end{aligned} \tag{3}$$

Here, subscripts i and 0 refer to the glacier and the rock, respectively; a denotes thermal diffusivity; $V_{iz}(z)$ is the vertical component of the ice flow velocity, which linearly decreases with depth from its maximal value V_s at the glacier surface to zero at the ice/rock boundary. The flow velocity at the glacier surface, $V_s = V_{iz}(-h)$, coincides with the accumulation rate. We assume that the temperature at the glacier surface, T_{is}, and the geothermal heat flow, q_0, are independent of time,

$$\begin{aligned} &T_i(-h, t) = T_{is}, \\ &\lambda_0 \frac{\partial T_0}{\partial z} = q_0 \quad \text{for} \quad z \to \infty \end{aligned}, \tag{4}$$

and the temperatures and heat flows in the two media are equal to each other at the ice/rock contact surface,

$$T_i(z, t) = T_0(z, t) \quad \text{and} \quad \lambda_i \frac{\partial T_i}{\partial z} = \lambda_0 \frac{\partial T_0}{\partial z} \quad \text{at} \quad z=0. \tag{5}$$

For times significantly exceeding the penetration time of the fastest "temperature signal" in the glacier, $t \gg \min(h/V_s, h^2/4a_i)$, the temperature distribution will become stationary everywhere:

$$\begin{aligned} T_{ist}(z) &= T_{is} + G_0 h \frac{\lambda_0}{\lambda_i} \frac{\sqrt{\pi}}{2} \frac{erf(\sqrt{Pe_m}) + erf(\sqrt{Pe_m}(z/h))}{\sqrt{Pe_m}} \\ T_{0st}(z) &= T_{is} + G_0 h \frac{\lambda_0}{\lambda_i} \frac{\sqrt{\pi}}{2} \frac{erf(\sqrt{Pe_m})}{\sqrt{Pe_m}} + G_0 z, \end{aligned} \tag{6}$$

Here, *erf(u)* is the error function, λ denotes thermal conductivity, $G_0 = q_0/\lambda_0$ is the geothermal gradient in the rocks corresponding to the geothermal heat flow q_0;

$Pe_m = V_{im} h / a_i$ is the ice Peclet number determined by the average flow velocity in the glacier $V_{im} = V_s/2$.

We tested the model using modern data on the HFD distribution, ice height, accumulation rates and surface temperature of the Greenland Ice Sheet (http://www.nsidc.org/data/gisp_grip/data/grip/physical/griptemp.dat, Dahl-Jensen et al., 1998). The model yields vertical temperature variations that agree well with the temperature-depth profiles from holes GRIP and Dye-3. Our calculations show that near GRIP the glacier warms up the rock by 8.5 K, while near Dye-3 it cools the rock down by 5.1 K due to a higher ice flow velocity. Thus, the presence of a glacier does not necessarily lead to a temperature increase at its base: a fast enough vertical ice flow can transfer low temperatures down from the outer surface. We calculated the warming influence of the Scandinavian and Kara's Ice Sheets for two regions: Kola Peninsula (near the Kol hole, 67.8° N) and Yamal Peninsula (near the holes Arctic, Nejtinsk-1 and Nejtinsk-2, 70° N). We used the initial parameters of the ice cover (thickness and accumulation rates) obtained within the QUEEN initiative (Quaternary Environment of the Eurasian North, Hubberten et al., 2004), which combined a number of numerical experiments and indirect paleoclimatic data sources. The initial data and our results are shown in Fig. 5 and Table 5.

The warming influence of the glacier was calculated relative to the average temperature of the upper layer of the rocks, which exceeds the surface air temperature by the magnitude of the warming influence of snow cover. Low heat flow on Kola Peninsula (30 mW/m^2) causes cooling of the upper layer of the rocks by 6.1 K, even though the accumulation rate is low, 0.12 m/year. On Yamal, with the same accumulation rate but a heat flow of 75 mW/m^2, the base of the glacier could warm up by 9.4 K. Although this number is close to the deviations of the PHW amplitude in the holes Arctic, Nejtinsk-1 and Nejtinsk-2 from the global distribution (12.8, 8.3 and 9.3 K, respectively), it hardly proves that the deviation from the regular pattern in the PHW amplitude distribution at the Arctic coast of Western Siberia is related exclusively to the warming influence of the Kara's Ice Sheet. The temperature changes caused by the glacier could leave a

significant trace in the modern temperature field only if they persisted for several tens of thousands of years – a period comparable to the time elapsed after the decay of the glacier. Besides, several tens of thousands of years are needed to reach the stationary conditions. At the same time, modern data show that the Kara's Ice Sheet was most developed during the Early and Middle Weichselian (90–60 thousand years back), and its decay occurred at the peak of the last glaciation period (Karabanov et al., 1998; Saarnisto, 2001; Velichko, 2002). The "glacier hypothesis" is even less convincing at explaining the Late Pleistocene warming in the lower Lena River. Most researchers agree that there was no developed Pleistocene glaciation in that region.

4.2 The influence of ice-dammed lakes

What, if not the ice sheets, could induce the anomalies in the distribution of geothermal estimates in Northern Siberia? Clearly, the relevant source of warming should be more powerful than the geothermal heat flow, and its duration longer than the lifetime of the ice sheets. The only possible such source is the Sun which creates a heat flow at the surface of the Earth of about 10^4 times larger intensity than the geothermal heat flow. However, within the time span under consideration there was no significant variation in solar activity, i.e. it only makes sense to look at possible re-distribution of solar energy. This idea is supported by the hypothesis of Karnaukhov (1994), according to which giant ice dams were formed in the mouths of the Ob, Yenisey and Lena Rivers during the ice ages. The ice broke up on these rivers in the South and accumulated in their mouths in the North forming the dams. The drainage interrupted, and large regions were flooded. The warming effect of this must have been significant because the flood water was already warmed up in the South. Similar but smaller-scale dams and floods occur now as well, their duration and scale increasing when the temperature drops and the latitude gradient of the mean annual temperature rises.

Ice-damming of lakes is mentioned also in the Panarctic Ice Sheet model (Hughes et al., 1977; Grosswald, 1996). In both hypotheses, a large-scale flooding of entire Western-Siberian lowlands was assumed. This could indeed be the case, but only dur-

ing a relatively short (in the geothermal sense) period of time – less than 10 thousand years. As for the period comparable to the duration of the ice age, about 70 thousand years, the flooding (continuous or periodic) only occurred in a smaller region within the identified anomalies of geothermal estimates, i.e. north of the 68-th parallel.

5 Discussion and conclusion

We identified two features in the spatial distribution of geothermal estimates of the Pleistocene/Holocene warming amplitude. (i) The amplitude decreases nonlinearly as a function of the distance to the hypothetical warming center. (ii) The latitude dependence of the estimates in Western Siberia and Yakutia north of the 68-th parallel exhibits inversion.

We explained the first, and major, feature by the influence of the system of warm currents in the North Atlantic. In Late Pleistocene there was no such anomaly, and hence no Gulfstream, North-Atlantic and Norwegian currents causing it, at least in their modern form. Probably the same sequence of events took place during the earlier ice ages of Pleistocene. Every time, a breakthrough of warm water from the South Atlantic to the North led to a sharp global warming. Further warming was caused by positive climatic feedback mechanisms, in particular, a decrease in the Earth albedo with shorter periods of snow cover.

Our second finding – the inversion of the latitude dependence of the estimates in Western Siberia and Yakutia north of the 68-th parallel – is also quite remarkable. The low estimates of PHW amplitudes for Arctic Siberia point at the existence of a sufficiently powerful and long-lasting warming factor, the origin of which is not entirely clear. We have shown that ice sheets or ice-dammed lakes could play a role in this. Perhaps, all the mentioned factors were at play at different periods in Late Pleistocene.

Our main conclusion is that the information extracted from geothermal data is sufficiently reliable, new, and independent from the existing set of paleoclimatic indicators. The climate system of the Earth will be understood better if all such indicators, including

the geothermal ones, are jointly taken into account.

Acknowledgements. This research was financially supported by the Integrated Project between the Urals and Siberian Branches of the RAS, "Reconstruction of the spatial distribution of Pleistocene-Holocene warming amplitudes in Northern Eurasia by geothermal data and RFBR-grant 06-05-64084."

References

Balobaev, V. T.: Geothermics of permafrost zone of the lithosphere of Northern Asia, Novosibirsk, Nauka, 194 pp. (in Russian), 1991.

Budyko, M. I.: Climate in the past and future, Leningrad, Gidrometeoizdat, 352 pp. (in Russian), 1980.

Dahl-Jensen, D., Mosegaard, K., Gundestrup, N., Clow, G. D., Johnsen, S. J., Hansen, A. W., and Balling, N.: Past temperature directly from the Greenland ice sheet, Science, 282, 268–271, 1998.

Demezhko, D. Yu. and Shchapov, V. A.: 80,000 years ground surface temperature history inferred from the temperature-depth log measured in the superdeep hole SG-4 (the Urals, Russia), Global and Planetary Change, 29(3–4), 219–230, 2001.

Demezhko, D. Yu.: Geothermal method for paleoclimate reconstruction (examples from the Urals, Russia), Russian Academy of Science, Ekaterinburg: Urals Branch, 143 pp. (in Russian), 2001.

Demezhko, D. Yu, Utkin, V. I., Shchapov, V. A., and Golovanova, I. V.: Variations in the Earth's Surface Temperature in the Urals during the Last Millennium Based on Borehole Temperature Data/Doklady Earth Sciences, 403(5), 764–766, 2005.

Demezhko, D. Yu., Utkin, V. I., Duchkov, A. D., and Ryvkin, D. G.: Geothermic Estimates of the Amplitudes of Holocene Warming in Europe, Transactions (Doklady) of the Russian Academy of Sciences/Earth Science Section, 407(2), 259–261, 2006.

Duchkov, A. D., Balobaev, V. T., Volodko, B. V., et al.: Temperature, permafrost and radiogenic heat production in the Earth's crust of Northern Asia, UIGGM SB RAS, Novosibirsk, 141 pp. (in Russian), 1994.

Glaznev, V. N., Kukkonen, I. T., Raevskii, A. B., and Jokinen, J.: New Data on Thermal Flow

in the Central Part of the Kola Peninsula, Transactions (Doklady) of the Russian Academy of Sciences/Earth Science Section, 396(4), 512–514, 2004.
Golovanova, I. V., Selezneva, G. V., and Smorodov, E. A.: Reconstruction of the warming after glaciation in the South Urals by the temperature measurements in boreholes, Geologitheskiy sbornik No 1, IG UB RAS, Ufa, p. 113–116 (in Russian), 2000.
Golovanova, I. V. and Valieva, R. Yu.: New estimates of paleoclimate change in the South Urals by the geothermal data, Proceedings of the III-d Scientific Readings in Memory of Yu. P. Bulashevich, Ekaterinburg, IGF UB RAS, p. 86–87, 2005.
Grosswald, M. G.: Evidence for a glacial invasion of the East Siberian coasts from the adjacent Arctic shelf, Doklady Akademii Nauk., 350(4), 535–540, 1996.
Huang, S., Pollack, H. N., Shen, P. Y.: Late Quaternary temperature changes seen in world-wide continental heat flow measurements, Geophys. Res. Lett., 24, 1947–1950, 1997.
Hubberten, H., Andreev, A., Astakhov, V., et al.: The periglacial climate and environment in northern Eurasia during the Last Glaciation, Quaternary Science Reviews, 23, 1333–1357, 2004.
Hughes, T. J., Denton, G. H., and Grosswald, M. G.: Was there a late Würm Arctic Ice Sheet, Nature, 266, 596–602, 1997.
Karabanov, E., Prokopenko, A., Williams, D., and Colman, S.: Evidence from Lake Baikal for Siberian Glaciation during Oxygen-Isotobe Substage 5d, Quaternary Research, 50, 46–55, 1998.
Karnaukhov, A. V.: Dynamics of glaciations in Northern Hemisphere as the process of self-oscillation and relaxation, Biophysics, 39(6), 1094–1098, (in Russian), 1994.
Kohl, T.: Palaeoclimatic temperature signals – can they be washed out?, Tectonophysics, 291, 225–234, 1998.
Kukkonen, I. T., Gosnold, W. D., and Šafanda, J.: Anomalously low heat flow density in eastern Karelia, baltic Shield: a possible paleoclimate signature, Tectonophysics, 291, 235–249, 1998.
Kukkonen, I. T. and Joeleht, A.: Weichselian temperatures from geothermal heat flow data, J. Geophys. Res., 108(B3), 2163, doi:10.1029/2001JB001579, 2003.
Payne, A. J., Huydrechts, P., Abe-Ouchi, A., et al.: Results from EISMINT model intercomparison: the effects of thermomechanical coupling, Journal of Glaciology, 46(153), 227–238, 2000.
Pollack, H. N., Hurter, S. J., and Johnson, J. R.: Heat flow from the Earth's interior: Analysis of

the global data set, Rev. Geophys., 31, 267–280, 1993.
Rajver, D., Šafanda, J., and Shen, P. Y.: The climate record inverted from borehole temperatures in Slovenia, Tectonophysics, 291, 263–276, 1998.
Saarnisto, M.: Climate variability during the last interglacial-glacial cycle in NW Eurasia, PAGES – PEPIII: Past Climate Variability Through Europe and Africa, August 27–31, Aix-en-Provence, France (http://atlas-conferences.com/c/a/h/i/79.htm), 2001.
Safanda, J. and Rajver, D.: Signature of the last ice age in the present subsurface temperatures in the Czech Republic and Slovenia, Glob. Planet Change, 29(3–4), 241–258, 2001.
Safanda, J., Szewczyk, J., and Majorowicz, J.: Geothermal evidence of very low glacial temperatures on a rim of the Fennoscandian ice sheet, Geophys. Res. Lett., 31, L07211, doi:10.1029/2004GL019547, 2004.
Serban, D. Z., Nielsen, S. B., and Demetrescu, C.: Long wavelength ground surface temperature history from continuous temperature logs in the Transilvanian Basin, Glob. Planet Change, 29(3–4), 201–218, 2001.
Siegert, M. J., Dowdeswell, J. A., Hald, M., and Svendsen, J.-I.: Modelling the Eurasian Ice Sheet through a full (Weichselian) glacial cycle, Global and Planetary Change, 31, 367–385, 2001.
Tarasov, L. and Peltier, W. R.: Greenland glacial history, borehole constraints, and Eemian extent, J. Geophys. Res., 108(B3), 2143, doi:10.1029/2001JB001731, 2003.
Velichko, A. A. (Ed.-in-chief): Dynamics of terrestrial landscape components and inner marine basins of the Northern Eurasia during the last 130 000 years, Atlas-monograph, Moscow, GEOS, 296 pp. (in Russian), 2002.

Table 1. The first group of estimates. Location of boreholes, PHW amplitude ΔT_s, references.

Num	Borehole	Location	Latitude, N	Longitude, E	ΔT_s	References
1	Fil-240	Romania	46° 23′	24° 38′	10	Serban et al. (2001)
2	Lj-1	Slovenia	46° 30′	16° 11′	10	Rajver et al. (1998)
3	Kirov-3000	Ukraine	48° 34′	32° 17′	12	Demezhko et al. (2006)
4	KTB	S-E Germany	49° 47′	12° 08′	9	Kohl (1998)
5	De-1	Czech Rep.	49° 49′	17° 23′	11	Safanda and Rajver (2001)
6	Udryn	N-E Poland	54° 14′	22° 56′	17	Safanda et al. (2004)
7	Il-1	S. Urals, Russia	55° 00′	60° 10′	8	Golovanova et al. (2000)
8	Le-1	S Urals, Russia	55° 40′	58° 35′	10	Golovanova and Valieva (2005)
9	SG-4	Mid. Urals, Russia	58° 24′	59° 46′	12	Demezhko and Shchapov (2001)
10	Krl	Karelia, Russia	63° 15′	36° 10′	18	Kukkonen et al. (1998)
11	Kol	Kola peninsula, Russia	67° 45′	35° 25′	20	Glaznev et al. (2004)
12	GRIP	Greenland	72° 36′	37° 39′ W	23	Dahl-Jensen et al. (1998)

Table 2. The second group of estimates. Location of boreholes, PHW amplitude ΔT_s, permafrost thickness change ΔH, references.

Num	Borehole	Latitude, N	Longitude, E	ΔT_s, K	ΔH, m	β, K/1000 years
Western Siberia						
1	Urengoy-1	66	79	10.4	150	0.58
2	Urengoy-2	66	79	12.3	160	0.68
3	Urengoy-3	66	80	10.3	125	0.57
4	Medvezhje-1	66	74	12.5	135	0.69
5	Medvezhje-2	66	74	12.7	170	0.70
6	Ermakovskaya	66	86	7.8	125	0.43
7	Kostrovskaya	66	86	8.8	145	0.49
8	Russkoye	67	80	9.2	100	0.51
9	Pestsovoye	67	75	10.2	120	0.57
10	Yamburg	68	75	8.7	105	0.48
11	Novy Port	68	72	2.5	35	0.14
12	Soleninskoye	69	82	5.3	45	0.29
13	Messoyakha	69	82	3.7	45	0.21
14	Arkticheskoye	70	70	0	0	0
15	Neytinskoye-1	70	70	4.5	35	0.27
16	Neytinskoye-2	70	70	3.5	45	0.19
17	Kharasavey	71	67	0	0	0
18	Kazantsevskaya	70	84	9.1	150	0.50
19	Dzhangodskaya	70	88	9.1	80	0.50
Yakutia						
20	Yakutsk	62	130	8.3	218	0.46
21	Kenkeme	62	129	8	210	0.44
22	Namtsy	63	130	7.2	100	0.4
23	Orto-Surt	63	125	8	95	0.44
24	Kyz-Syr	64	124	10.3	107	0.57
25	Nedzheli	64	126	11.8	127	0.65
26	Sobo-Khaya	64	127	9.9	270	0.49
27	Balagatchi	65	124	8.6	60	0.48
28	Bakhynay	66	123	7.4	70	0.41
29	Viluisk	64	123	10.7	130	0.53
30	Promyshlenny	64	126	7.6	210	0.4
31	Govorovo	71	127	−2.3	−40	
32	Dzhardzhan	68	124	13.3	50	
33	Ust-Viluy	64	126	7.6	210	
34	Sr.-Viluy	64	124	9.8	83	
35	Oloy	63	126	9.8	140	
36	Borogontsy	63	132	7.2	100	

Table 3. The sample of PHW amplitude estimates prepared for the model parameters determination.

Num	Table num., data num	Num of estimates	Location	ΔT_s, K
1	1: 1	1	Romania	10
2	1: 2	1	Slovenia	10
3	1: 3	1	Ukraine	12
4	1: 4, 5	2	Germany, Czech Rep.	10
5	1: 6	2	Poland	17
6	1: 7, 8	1	S. Urals	9
7	1: 9	1	Mid. Urals	12
8	1: 10	1	Karelia	18
9	1: 11	1	Kola peninsula	20
10	1: 12	1	Greenland	23
11	2: 1–3, 8	4	W. Siberia	10.6
12	2: 4, 5, 9	3	W. Siberia	11.8
13	2: 6, 7	2	W. Siberia	8.3
14	2: 23–30, 33–35	11	Yakutia	9.2
15	2: 20–22, 36	4	Yakutia	7.7

Table 4. Parameters of the model of PHW amplitude spatial distribution.

Model	n	m	Variance D, K^2	M=1-R^2	$(DM)^{1/2}$, K	Coefficients		Coordinates of the center	
						k_1	k_2	Latitude, N	Longitude, E
S1	15	1	21.72	0.1522	1.82	26.91	$-4.6230\ 10^{-3}$	74.94°	12.32°
S2	15	−1	21.72	0.0916	1.41	1.75	$2.7141\ 10^{4}$	71.12°	0.31°
S3	15	−2	21.72	0.0974	1.45	7.15	$2.9999\ 10^{4}$	69.05°	0.80°

Table 5. Initial conditions and calculated ice-sheet temperatures.

	Kola	Yamal
Initial conditions		
Initial basal temperature (mean annual air temperature), ˚C	−23	−25
Ice sheet thickness, m	2100[(1)]	750[(2)]
Accumulation rate, m/year	0.12[(3)]	0.12[(3)]
Mean ice conductivity: λ_i=9,828exp(−0,0057T_{avg}), W m^{-1}K^{-1}[(5)]	2.46	2.33
Bedrock conductivity, W m^{-1}K^{-1}	2.8[(5)]	2.0
Geothermal heat flow $q=\lambda_i G_i$, mW m^{-2}	30[(5)]	75[(6)]
Vertical air temperature gradient, Ga, K/m	0.0065	0.0065
Initial conditions for air/ground temperature difference calculation (snow cover influence)[(7)]		
Mean annual air temperature, ˚C	−23	−25
Annual air temperature amplitude (T_{Jul}−T_{Jan})/2, K	15	20
Snow conductivity, W m^{-1}K^{-1}	0.46	0.46
Snow diffusivity, m^2/s X10^{-6}	0.55	0.55
Maximum mean decade snow thickness, m	0.6[(8)]	0.3[(8)]
Air/ground temperature difference (snow cover influence), K	+6	+4.5
Calculated parameters		
Stationary temperature gradient at the ice sheet basement G_i, K/m	0.0122	0.0341
Stationary temperature at the ice sheet basement, ˚C	−23.1	−11.7
Warming/cooling influence of the ice sheet, K	−6.1	+9.4

Comments:
(1) The maximal value of the ice sheet thickness obtained from the models *ISM* (Siegert et al., 2001) and *AGCM* (Hubberten et al., 2004) was used.
(2) From the model *AGCM* (Hubberten et al., 2004).
(3) The minimal value of the accumulation rate from the model *AGCM* (Hubberten et al., 2004)
(4) Tarasov and Peltier (2003)
(5) Glaznev et al. (2004)
(6) Duchkov et al. (1994)
(7) The algorithm proposed by Demezhko (2001)
(8) Contemporary values of maximum mean decade snow thickness were used.

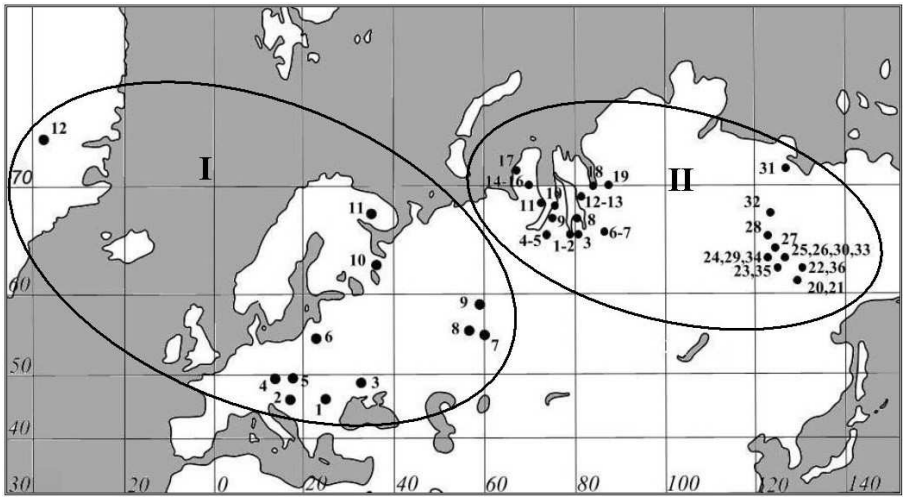

Fig. 1. Locations of the geothermal estimates of Pleistocene-Holocene warming (PHW) amplitude. Numbers next to the estimates are the same as in Table 1.

CPD
3, 607–630, 2007

EGU

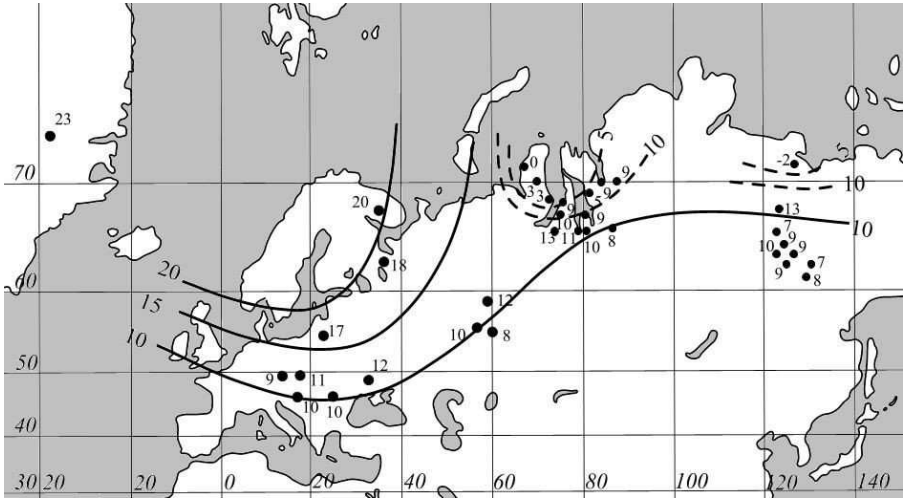

Fig. 2. The spatial distribution of the geothermal estimates of PHW amplitude in Northern Eurasia (K). Solid lines represent the main pattern the distribution follows; dashed lines show local anomalies.

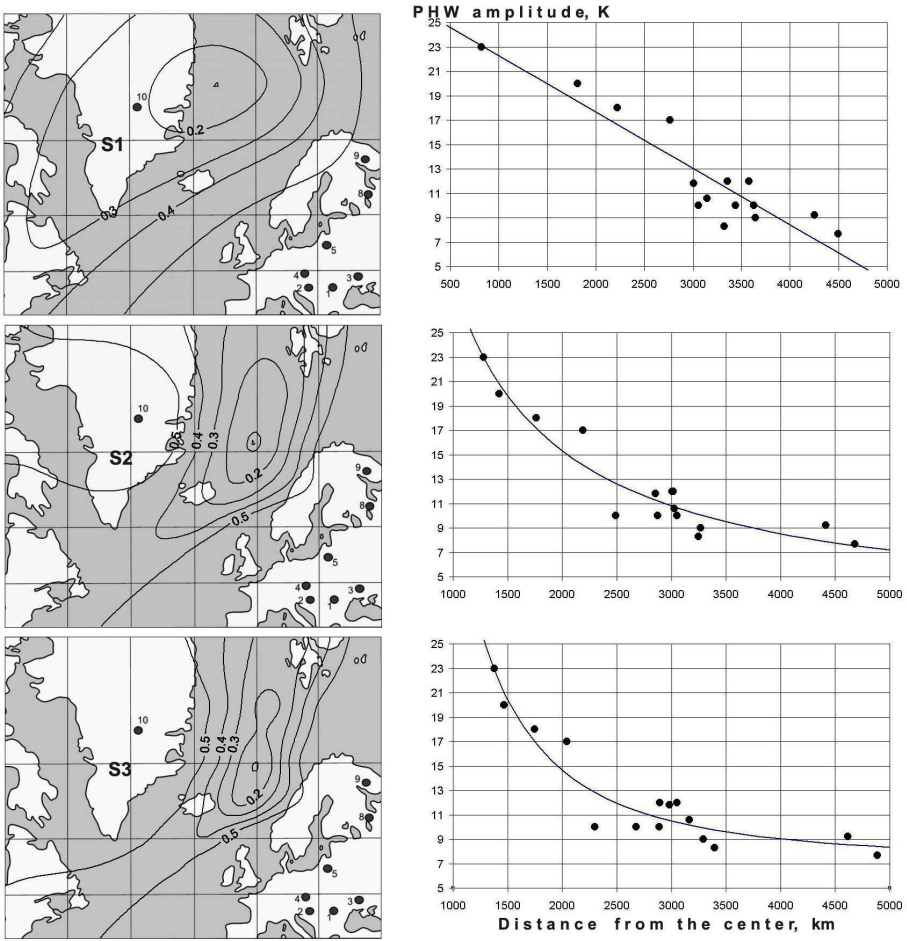

Fig. 3. Isolevel surfaces of functional $M(\varphi_0, \lambda_0)$ (left panels), and the dependence of PHW amplitude on the distance from the center of warming (right panels) for models S1–S3.

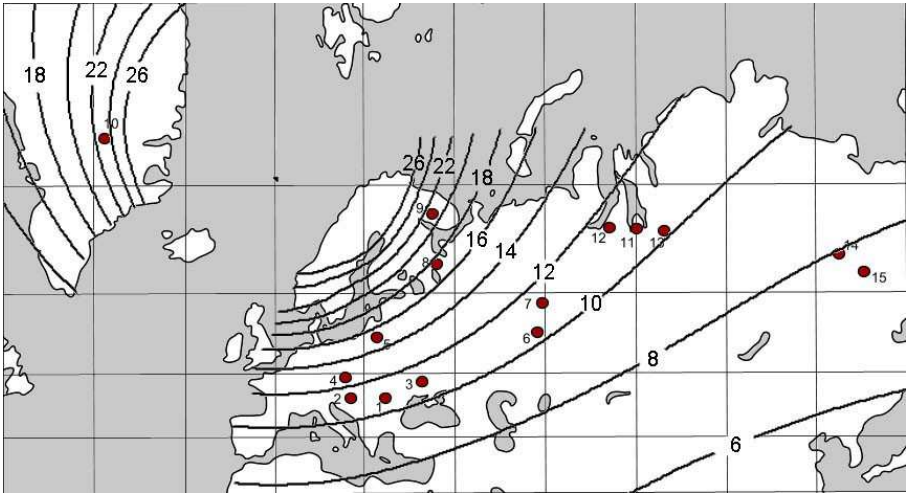

Fig. 4. The spatial distribution of PHW amplitudes in Northern Eurasia (K) according the model S2. Numbers next to the estimates are the same as in Table 3.

CPD
3, 607–630, 2007

EGU

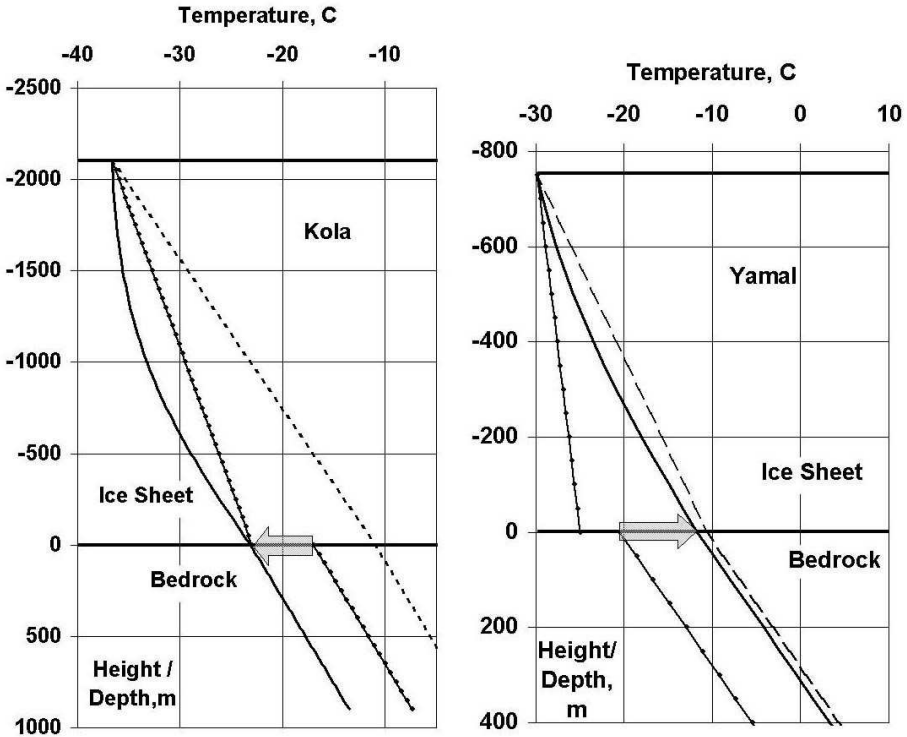

Fig. 5. The Influence of Late Pleistocene ice sheets on the basal temperature. The solid lines with points show the initial temperature distribution; the dashed lines show the stationary temperature distribution with no vertical ice advection; the solid lines show the stationary temperature distribution with vertical ice advection.